JOURNAL OF MATERIALS SCIENCE **34** (1999) 497–508

Composition-dependent properties of polyethylene/Kaolin composites

Part II *Thermoelastic behaviour of blow-moulded samples*

V. P. PRIVALKO*, F. J. BALTA CALLEJA
Instituto de Estructura de la Materia, CSIC, Serrano 119, 28006 Madrid, Spain
E-mail: embalta@iem.csic.es

D. I. SUKHORUKOV, E. G. PRIVALKO
Institute of Macromolecular Chemistry, National Academy of Sciences of Ukraine, 253160 Kyiv, Ukraine

R. WALTER, K. FRIEDRICH
Institute of Composite Materials Ltd., University of Kaiserslautern, D-67663, Kaiserslautern, Germany

Samples of the blow-moulding grade HDPE filled with Kaolin were characterized by wide-angle X-ray scattering, microhardness and stretching calorimetry techniques. It is shown that crystallinity of the polymer matrix in the filled samples remains essentially the same as that in the neat polymer regardless of the filler content. The thermoelastic behaviour of all samples below the apparent yield point ε^* is quantitatively described by classical equations for elastic solids. The thermoelastic parameters of the boundary interphase (BI) are discussed in terms of predictions of the step-by-step averaging approach. The experimental values of the internal energy increment in the inelastic strain interval for unfilled and filled samples are analyzed in the light of the filler debonding processes in the latter.

1. Introduction

The incorporation of rigid fillers in a thermoplastic polymer often results in an enhancement of stiffness, but at the cost of a reduced strength and/or toughness. However, as shown [1, 2] in recent studies of high-density polyethylene (HDPE)/Kaolin melt-blended composites, the stiffness enhancement is not necessarily accompanied by a reduction in strength, especially when an appropriate coupling agent is used. Kaolin-filled samples of both blow-moulding and injection-moulding HDPE grades exhibited a good dispersion of filler particles and essentially the same crystallinity of the polymer matrix as that of the neat polymer; in addition, stiffness and toughness were also improved.

The data available [1, 2] clearly highlight the importance of the bonding quality at the polymer/filler interface in the mechanical performance of the composites. However, up till now a quantitative characterization of the micromechanics of composite deformation is still missing. The main purpose of the present study is to obtain relevant thermoelastic data by using the stretching calorimetry technique.

2. Experimental

2.1. Materials

A blow moulding grade (melt flow index MFI = 0.27 g/10 min) of high-density polyethylene (hereafter referred to as HDPE 2) was used as a matrix. Filled composites prepared on a twin-screw extruder by compounding the polymer matrix with Kaolin particulates (mean size 0.8 and 1.4 μm for Short and Long particles, respectively) and a custom coupling agent were supplied by the manufacturer (ENICHEM, Italy). Kaolin with the formula $Al_2O_3 \cdot SiO_2 \cdot 2H_2O$ was calcinated by heating above 600 K. This treatment is assumed [3] to improve the catalytic activity of the Kaolin surface and to destroy its crystalline structure.

Samples with lateral dimensions of 5×50 mm^2 cut from 0.3 mm-thick sheets in longitudinal (L) and transversal (T) direction (with respect to the mould filling direction) were used for subsequent structural and thermoelastic characterization. As an example, the sample coding 10 BYS-L means: 10 vol % of the Kaolin, Blow moulding grade of the matrix, presence of the coupling agent (Yes), Small Kaolin particles, Longitudinal orientation.

* *Permanent address*: Institute of Macromolecular Chemistry, National Academy of Sciences of Ukraine, 253160 Kyiv, Ukraine.

2.2. Techniques

Wide-angle X-ray scattering (WAXS) patterns in the 5–40° scattering angle range (2Θ) were taken using a DRON-2,0 diffractometer (CuK_α radiation with Ni filter was used). The WAXS patterns were recorded in the stepwise scanning mode using a scintillation counter and digital conversion. The scattering curves for all samples were normalized by thickness and X-ray absorption [4, 5].

A Leitz Tester equipped with a square-based diamond indenter was used for the microhardness (H) measurements. The H values were calculated from the standard equation [6, 7], H (MPa) $= kS$, where S is the slope of the straight-line plot of the residual projected indentation area $A\,(m^2) = d^2$ vs. the contact load applied P (N), d (m) is the diagonal length of the impression, and $k = 1.854$ is the geometrical factor. In a loading cycle of 0.1 min the loads of 0.5, 1 and 1.5 N were used. For each point, at least 3–5 measurements were averaged. The correlation coefficients and the standard deviations for the linear A vs. P fits obtained were 0.998 and 1.16, respectively.

The mechanical work (W) and concomitant heat effects (Q) in the stepwise loading (stretching)/unloading (contraction) cycles were measured (with the estimated mean error below 2%) at room temperature with the stretching calorimeter described in detail elsewhere [8–11]. In every experimental run, each specimen was stretched at a constant velocity q^+ to a predetermined strain ε_i, stored at fixed ε_i to the full completion of mechanical and thermal relaxations, and thereafter allowed to contract at the same velocity q^- to zero force. The typical difference between fixed strains in two successive steps, $\varepsilon_{i+1} - \varepsilon_i$, varied from several digits in the fourth place to a few digits in the third place within the strain intervals below and above 0.02, respectively. In the large-strain interval (above 0.1), the data were taken in the stretching regime only. Successive step-like strains increased with stretching ratio from about 0.05–0.10 up to 0.15–0.20.

3. Results and discussion

3.1. Structure and microhardness

The overall WAXS pattern as well as the angular positions of crystalline peaks of the polymer matrix (Fig. 1) correspond to those for a semi-crystalline HDPE (e.g. [12, 13]). The same WAXS pattern is also observed in filled samples (Fig. 2). The absence of extra WAXS reflections due to Kaolin confirms its assumed [3] non-crystalline structure. As expected, the WAXS intensities decrease with increasing filler volume content φ (Fig. 2). However, the degree of crystallinity estimated by the standard procedure [4, 12, 13] compares well

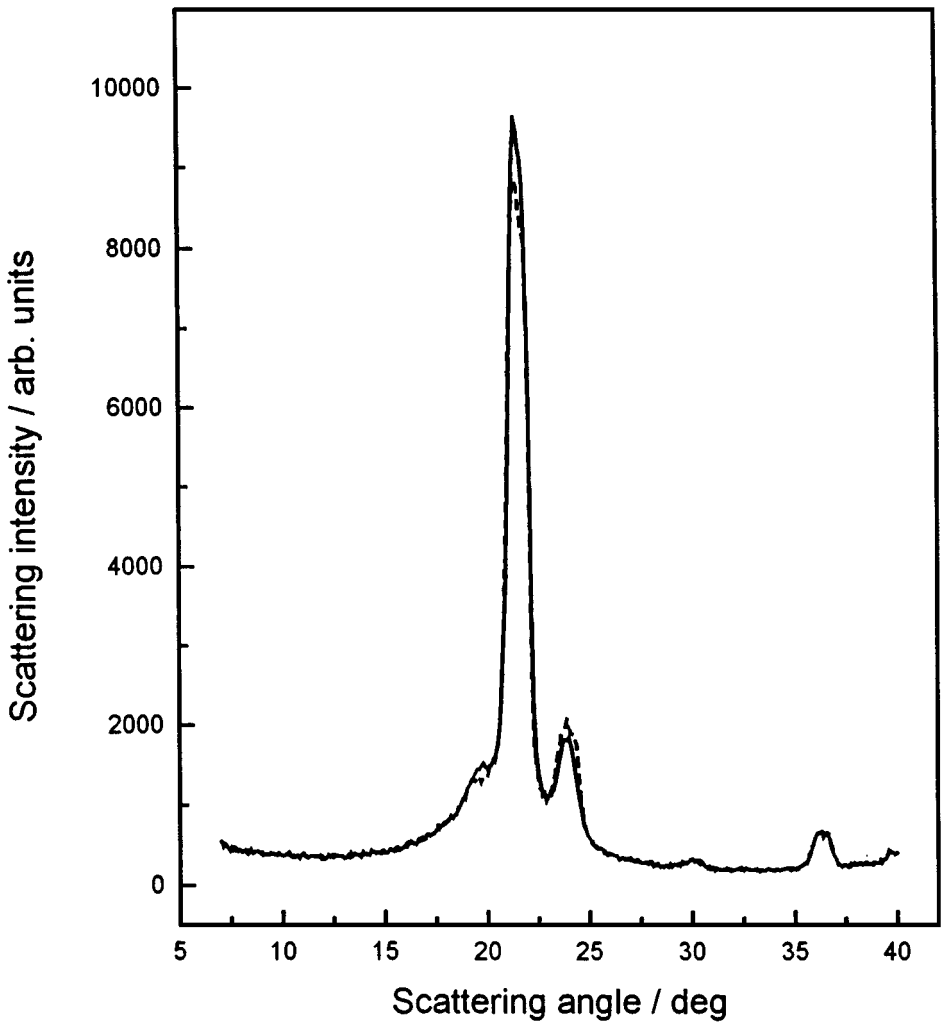

Figure 1 Wide-angle X-ray scattering patterns for HDPE 2-L (solid line) and HDPE 2-T (broken line).

TABLE I Microhardness and thermoelastic parameters of the studied samples

Sample	H (MPa)	E (GPa)	$\alpha_L \cdot 10^5$ K^{-1}	ε^*	ε_b	C	$\Delta U/m$ (J kg^{-1})	f
HDPE 2-L	49.1	0.74	9.9	0.019	1.10	3.5	1070	—
HDPE 2-T	45.4	0.45	13.5	0.032	0.65	3.1	1280	—
10 BYS-L	63.6	0.85	9.6	0.023	1.02	3.2	910	0.07
10 BYS-T	56.3	0.72	10.5	0.024	0.49	3.2	1130	0.06
30 BYS-L	67.2	1.30	7.6	0.019	0.44	2.7	630	0.18
30 BYS-T	66.3	1.26	6.6	0.020	0.25	2.6	880	0.17

with those estimated by calorimetry [2] and remained constant ($X = 0.62 \pm 0.03$) irrespective of the sample composition and/or orientation.

The microhardness values H_1 of HDPE 2-L and HDPE 2-T (Table I) are close to those for semicrystalline HDPE with small crystal size [14]. It can be easily verified that the observed increase of H with Kaolin content φ for both L- and T-series (Table I) fits reasonably well to a straight line intersecting the ordinate ($\varphi = 1.0$) at $H_2 = 110 \pm 4$ MPa. The intercept should be regarded as the microhardness of bulk Kaolin (unfortunately, the experimental value of H for bulk Kaolin is not available). The tabulated value of the Moh's hardness for Kaolin ($M = 2.3$ [15]) can be converted into the Vickers hardness $H_2' = 575$ MPa using the empirical relationship H (MPa) $= 192.7 \exp(0.476\ M)$ (derived by treatment of the relevant data from Table 10 in Tabor's book [16]).

The large difference between the extrapolated H value and the one derived from Moh's hardness for Kaolin has no immediate explanation at the moment. However, the five-fold lower value of the former might be related to the effect of amorphization of the virgin, polycrystalline (hence, presumably much harder) bulk Kaolin.

3.2. Thermoelasticity

3.2.1. Elastic strains range

In the interval of small strains ($\varepsilon \leq 0.025$) the specific (per sample mass m) mechanical work (W/m) and specific heat effects (Q/m) data for both HDPE 2-L

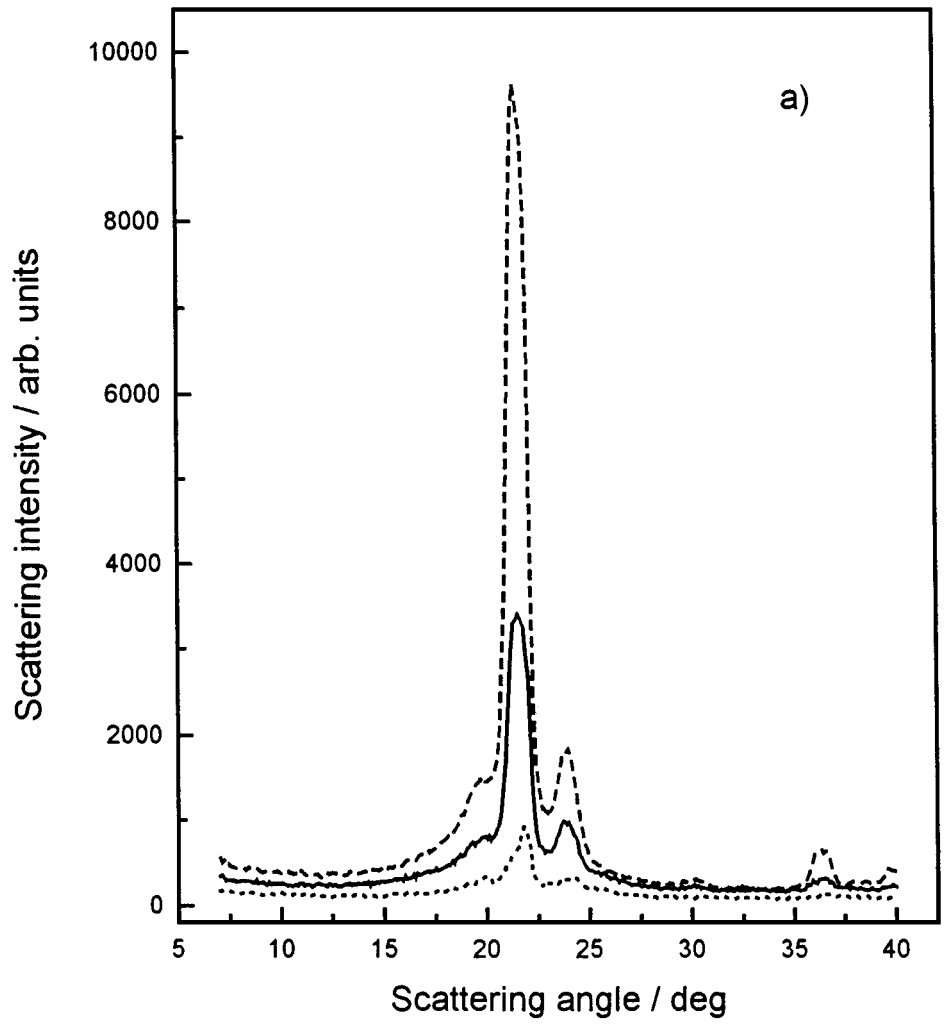

Figure 2 Wide-angle X-ray scattering patterns for samples of series L (a): HDPE 2-L (broken line), 10 BYS-L (solid line) and 30 BYS-L (dotted line), and for samples of series T (b): HDPE 2-T (broken line), 10 BYS-T (solid line) and 30 BYS-T (dotted line). (*Continued*).

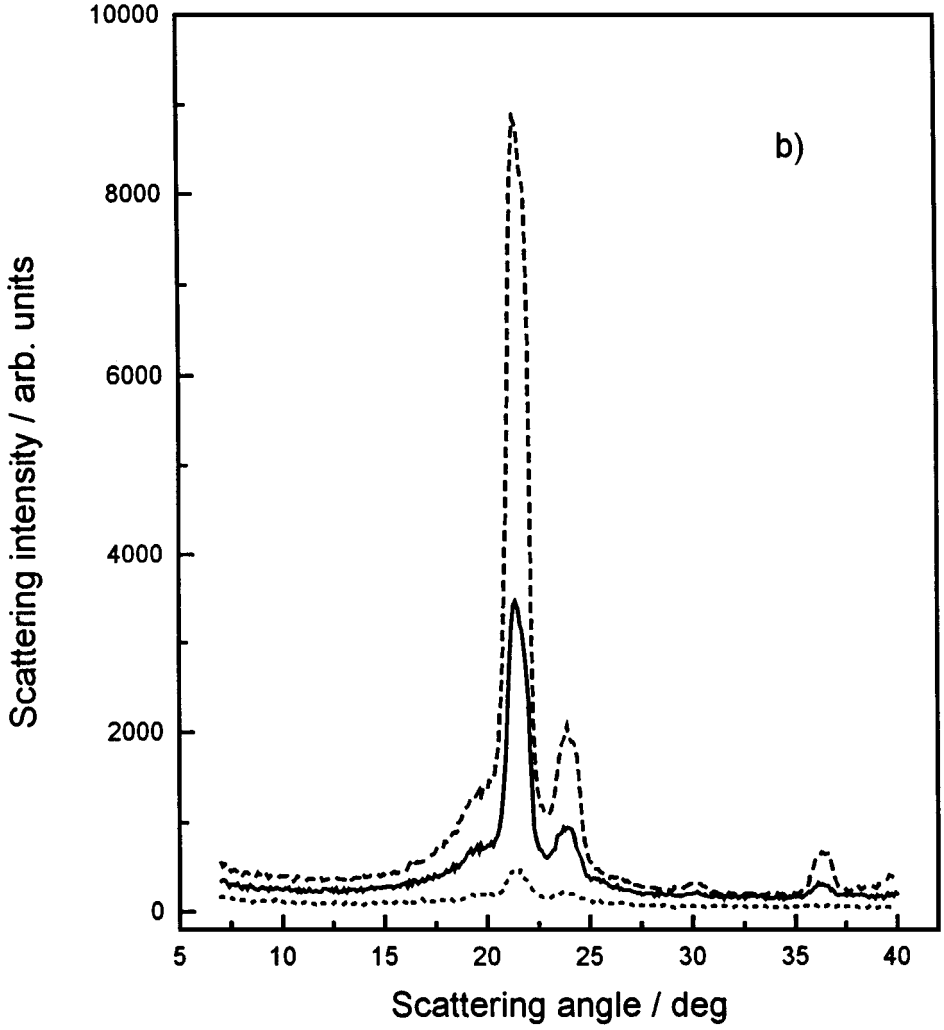

Figure 2 (*Continued*).

and HDPE 2-T can be quantitatively fitted (Fig. 1) to the classical equations of the thermoelasticity of solids [17]

$$W/m = E\varepsilon^2/2\rho; \quad (1a)$$

$$Q/m = E\alpha_L T\varepsilon/\rho \quad (1b)$$

where E is the Young's modulus, α_L is the linear expansion coefficient and ρ is the density. As can be seen from Table II, the values of E and α_L for HDPE 2-L are respectively higher and smaller than those for HDPE 2-T. Since the crystallinity for both samples is nearly the same, the observed differences can be attributed [17] to the somewhat more strained conformation of tie-chains in the interlamellar space of HDPE 2-L.

Equations 1 proved also applicable to describe the experimental data for filled samples at low strains (Figs 3 and 4); the best-fit values of Young's moduli E and linear expansion coefficients α_L are collected in Table I. The observed trend for the E increase and for the α_L decrease with filler content φ is a consequence of a much higher Young's modulus and of a much lower linear expansion coefficient of bulk polycrystalline kaolin ($E_2 \approx 20$ GPa and $\alpha_{L,2} \approx 1 \times 10^{-6}$ K^{-1}, respectively [18]) as compared to those for the neat matrix polymer. The essentials of the step-by-step averaging (SSA) approach [19] which will be used for a quantitative treatment of these data are outlined below.

A unique feature of the structural model adopted in the SSA [19] is the possibility to explicitly account for the smearing out of a sharp ("mathematical") interface between a filler and a matrix polymer into a "physical" boundary interphase (BI) structurally different from the neat polymer. It is assumed that even at relatively low nominal values of φ the isolated filler particles of size $2r$ coated with a BI of thickness Δr can coalesce into isolated clusters (IsC) containing a constant limiting volume fraction of a filler $\varphi^* \gg \varphi$. The effective concentration φ' of such IsC with $\varphi^* = \text{const}$ will increase with the nominal filler content φ until an infinite cluster (InC) spanning the entire system is formed at the percolation threshold $\varphi' = \varphi_c$. The bulk representative elements (BRE) of the InC are Voronoi polyhedra constructed by the intersection of planes drawn normal to the vectors connecting the centres of particles at their midpoints. In this fashion, the InC is sectioned into a system of different Voronoi polyhedra with the number of faces dependent on the coordination number $N_c = f(\varphi^*)$ of corresponding particles. The effective properties of a disordered system of such BRE are calculated assuming its identity to the appropriately chosen, "mutually adequate" (as concerns isotropicity, mechanical stability, geometrical equivalence, etc.) one with an

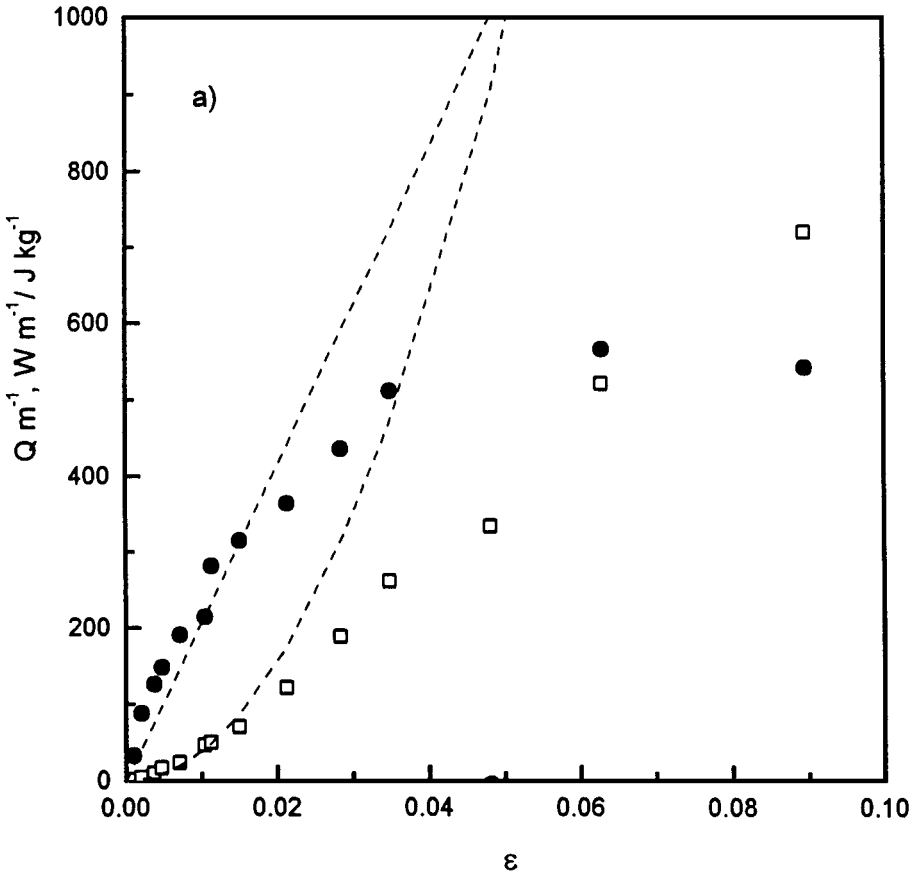

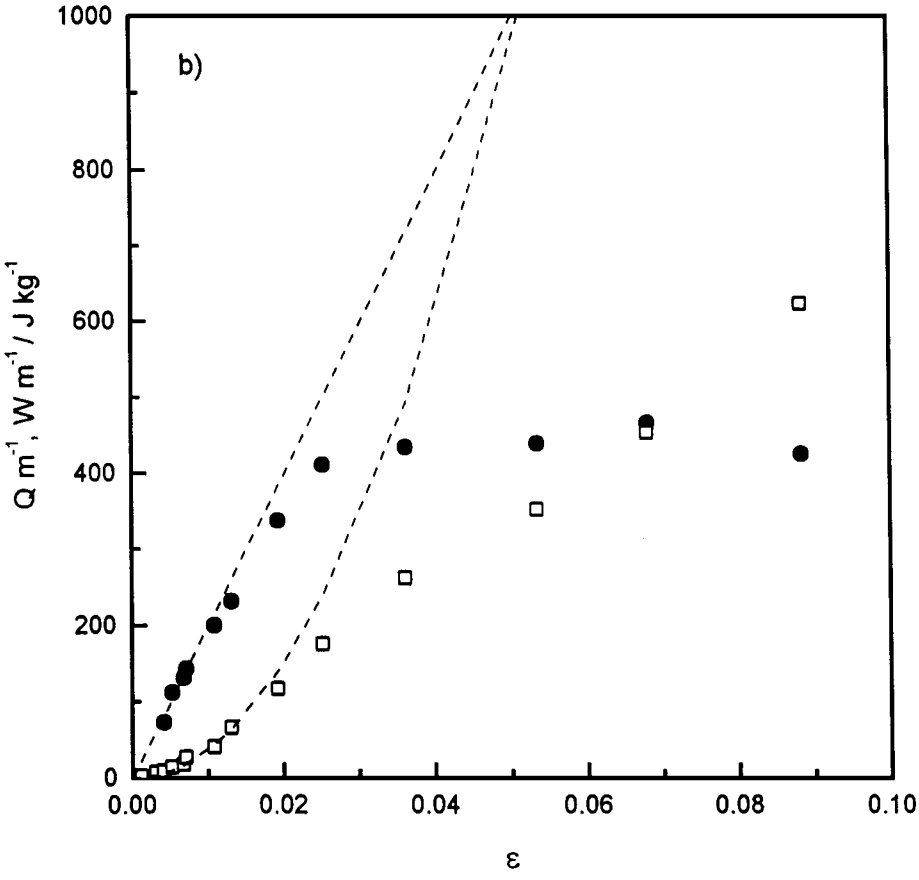

Figure 3 Specific mechanical work (opened squares) and specific heat effect (filled circles) for HDPE 2-L (a), 10 BYS-L (b) and 30 BYS-L (c). (*Continued*).

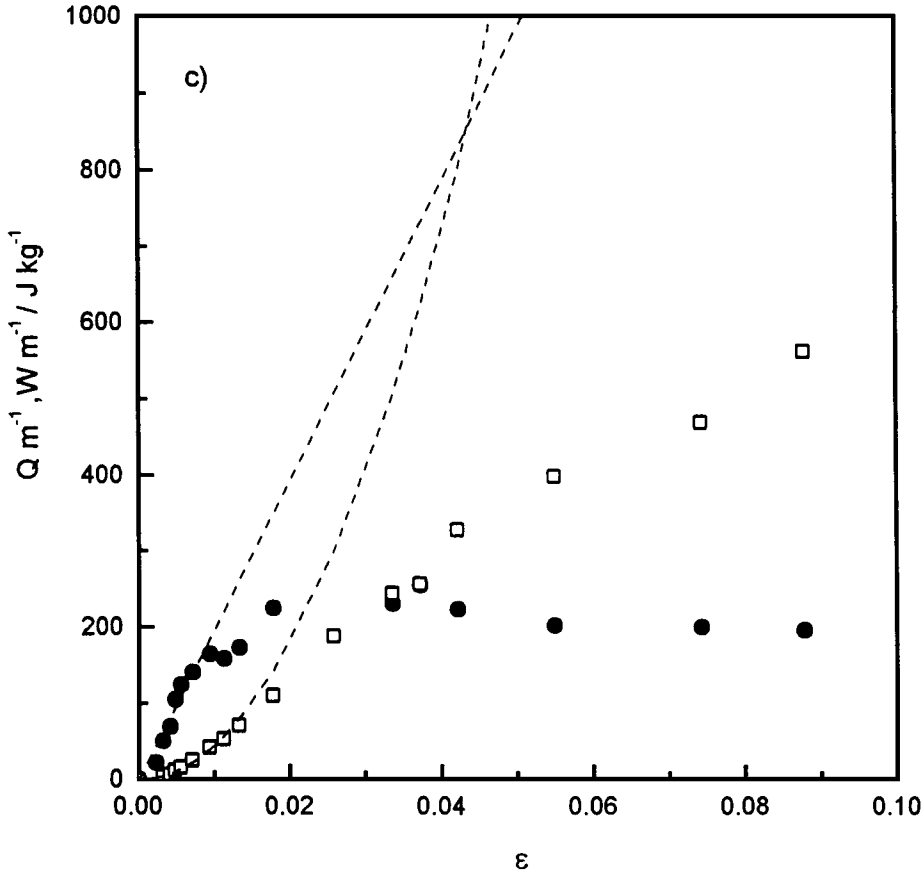

Figure 3 (*Continued*).

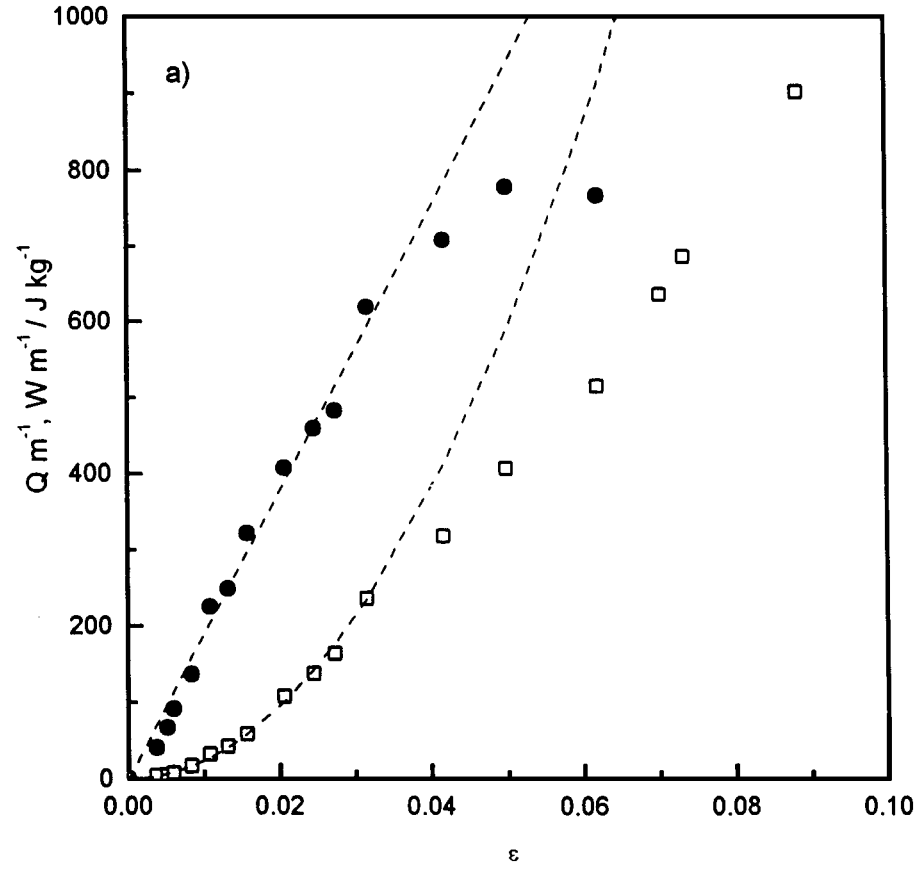

Figure 4 Specific mechanical work (opened squares) and specific heat effects (filled circles) for HDPE 2-T (a), 10 BYS-T (b) and 30 BYS-T (c). (*Continued*).

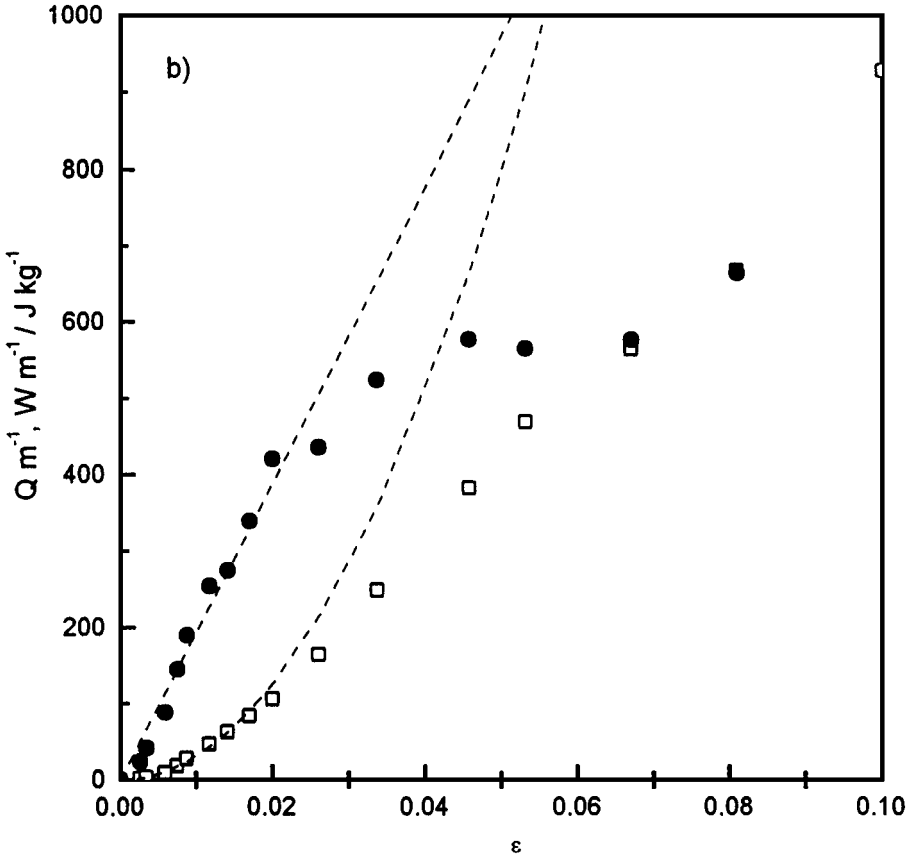

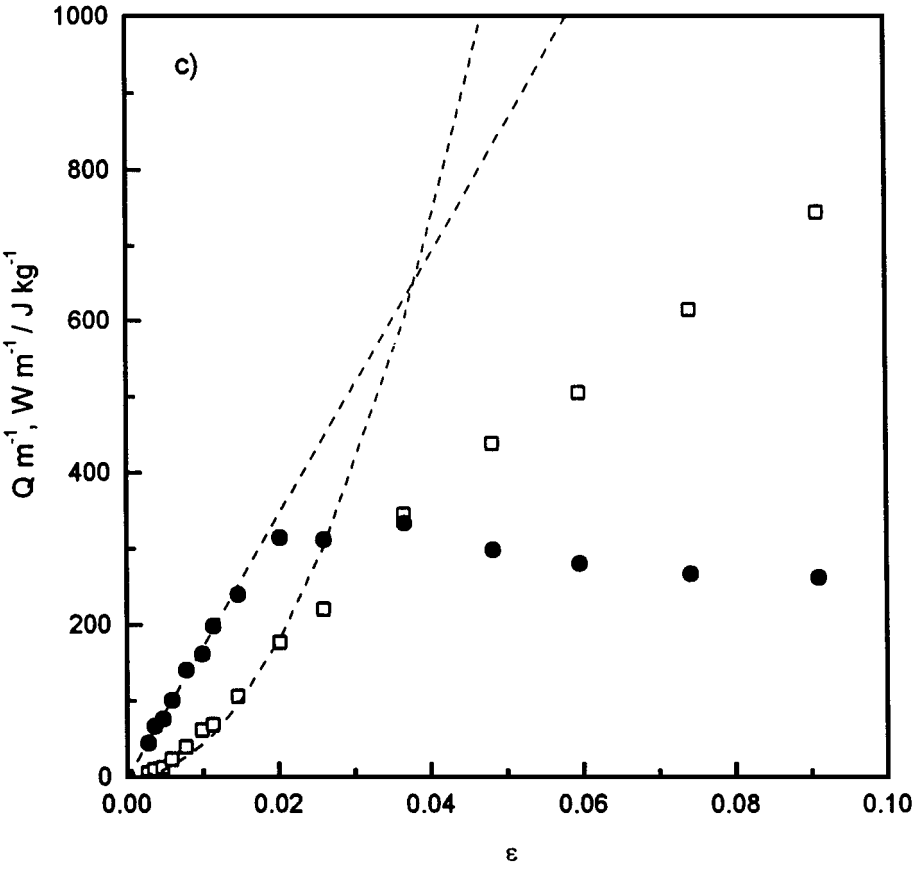

Figure 4 (*Continued*).

ordered structure (e.g. a spherical particle embedded into a cube).

Calculations were carried out for different values of the effective Young's modulus and linear expansion coefficient of the BI (E_{BI} and $\alpha_{L,BI}$, respectively) at fixed values of $\varphi_c = 0.15$, $\varphi^* = 0.60$, $\nu_1 = 0.4$ and $\nu_2 = 0.2$ (the latter two parameters are Poisson's ratios of the matrix polymer and of kaolin, respectively).

The agreement between theoretical and experimental Young's moduli for both L- and T-series (Figs 5a and 6a) as well as the linear expansion coefficients of the T-series (Fig. 6b) proves to be reasonably good (at the best-fit values $E_{\mathrm{BI}} = 10.74$ GPa and 10.45 GPa for L- and T-series, respectively, and $\nu_{\mathrm{BI}} = 0.4$ and $\alpha_{\mathrm{L,BI}} < 1 \times 10^{-7}$ K^{-1} for both series), whereas larger discrepancies are observed for linear

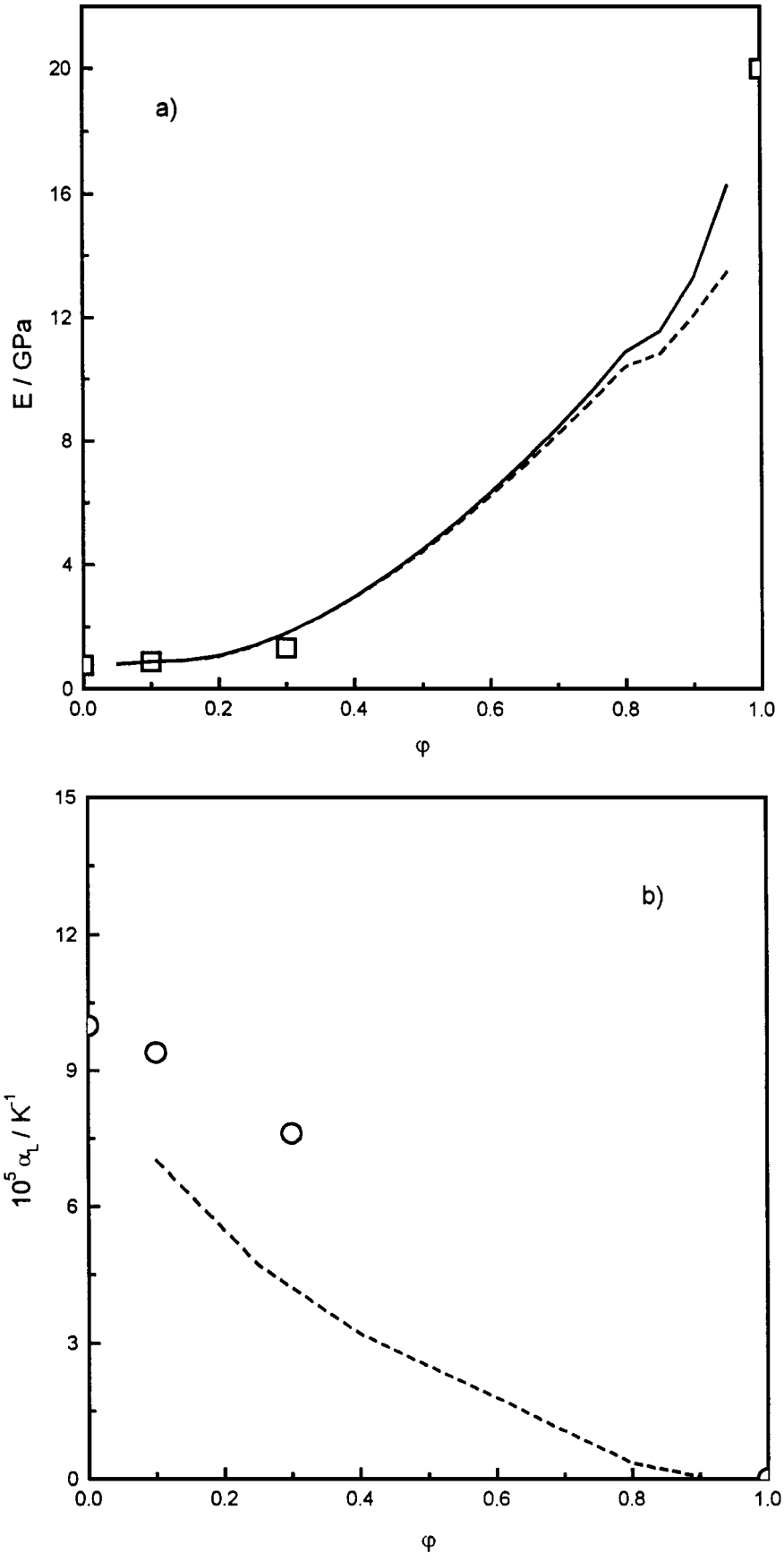

Figure 5 Concentration dependences of Young's modulus (a) and linear expansivity (b) for samples of series L. Theoretical curves were calculated assuming $\Delta r/r = 0.01$ (solid lines) and 0.001 (broken lines).

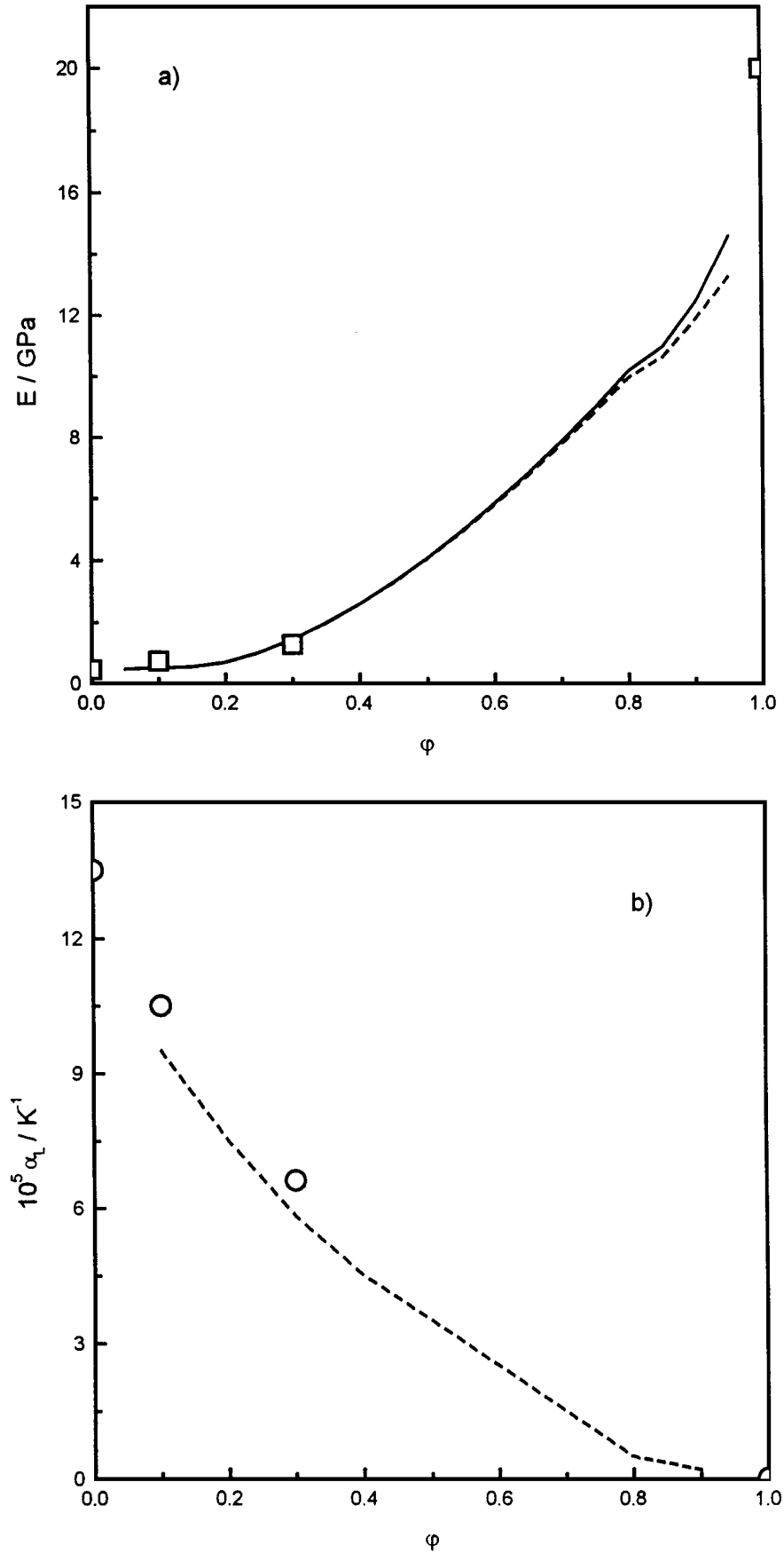

Figure 6 Concentration dependences of Young's modulus (a) and linear expansivity (b) for samples of series T. Theoretical curves were calculated assuming $\Delta r/r = 0.01$ (solid lines) and 0.001 (broken lines).

expansion coefficients of the L-series (Fig. 5b). As expected /18/, the change of the effective BI thickness $\Delta r/r$ by an order of magnitude produces only a minor effect on the fit to the experimental E data (Figs 4a and 5a), and does not affect the theoretical curves of α_L (Figs 5b and 6b).

The effective E_{BI} and $\alpha_{L,BI}$ values (if real) would imply an unusually stiff, highly oriented state of HDPE 2

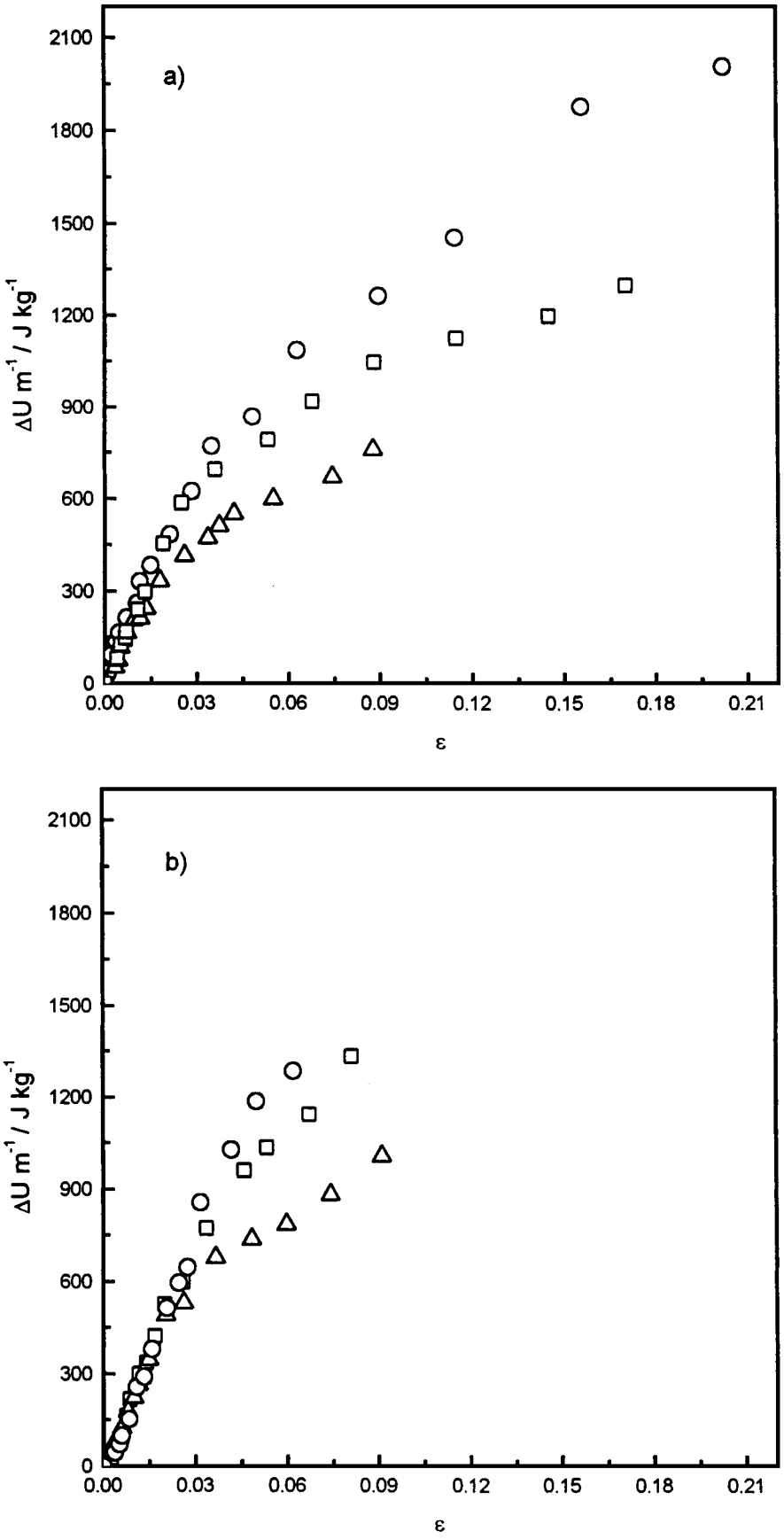

Figure 7 Specific internal energy changes for samples of series L (a): HDPE 2-L (circles), 10 BYS-L (squares) and 30 BYS-L (triangles), and for samples of series T (b): HDPE 2-T (circles), 10 BYS-T (squares) and 30 BYS-T (triangles), and for samples of series T (b).

in the BI of filled samples (the representative values of $E = 8.0$ GPa and $\alpha_L = -3.65 \times 10^{-5}$ K^{-1} were reported /17/ for a sample of HDPE stretched 20-fold). This is a necessary requirement for the fit of the experimental values of thermoelastic parameters of the filled samples to predictions of the SSA model over the entire concentration interval from neat HDPE to a polycrystalline Kaolin (Figs 4 and 5). Since thermoelastic

parameters of an amorphized Kaolin are lacking, it is impossible at the moment to arrive at more realistic values of E_{BI} and $\alpha_{L,BI}$ from our model calculations.

3.2.2. Inelastic strain range

As can be seen from Figs 3 and 4, the fit of experimental data to theoretical Equations 1 for elastic solids is limited to a relatively narrow strain interval below the apparent yield strain ε^*. The increasing deviation of experimental data from theoretical curves at higher strains suggest the onset and subsequent development of irreversible (inelastic) structural changes within the samples (commonly referred to as a "plastic flow" phenomenon).

At this point it is worth to mention that the data of Table I are consistent with the expected [6] correlation between the microhardness, H, and the apparent yield stress, $\sigma^* = E\varepsilon^*$. As can be seen from Table I, the proportionality coefficients C in the relationship, $H = C\sigma^*$, for both L- and T-series are reasonably close to the theoretical value ($C = 3$) for compression loading of solids [6], and tend to decrease, the higher the filler content.

Let us discuss next the structural implications of thermoelastic behaviour of studied samples in the strain interval of plastic flow above ε^* with reference to the specific internal energy change, $\Delta U/m = (W + Q)/m$. As can be seen from Fig. 7, the initial steep increase of $\Delta U/m$ with ε for both HDPE 2-L and HDPE 2-T in the interval of elastic strains ($\varepsilon < \varepsilon^*$) is followed by a gradual decrease of the slope of $\Delta U/m$ in the strain interval above ε^*. According to current views [17], this behaviour can be explained by the elastic (endothermic) response of the tie-chains connecting randomly oriented lamellar crystals in the initial isotropic sample in the interval $\varepsilon < \varepsilon^*$, and by the onset of successive (exothermic) processes of lamella reorientation and breakdown at higher strains, respectively.

The overlap of experimental data for unfilled and filled samples of both series in the interval $\varepsilon < \varepsilon^*$ (Fig. 7) suggests the occurrence of similar structural mechanisms responsible for their thermoelastic behaviour (i.e., the elastic response of tie-chains between crystalline lamellae in the polymer matrix). However, for filled samples the $\Delta U/m$ values at equal strains in the interval $\varepsilon > \varepsilon^*$ are significantly smaller than those for the corresponding neat polymer, and tend to decrease with filler content. This can be regarded as experimental evidence for extra exothermic processes of structural reorganization in the filled samples, the contribution of which increases when the filler content is higher.

As can be seen from Table I, the irreversible (inelastic) structural changes within filled samples start at systematically lower values of the apparent yield strain ε^* as compared to corresponding neat polymers. The decrease of breaking strain ε_b with filler content is even more dramatic. Qualitatively, the former effect implies higher (compared to a near polymer) local strains within polymer interlayers (ligaments) between neighbouring filler particles, whereas the latter one can be explained by the increased probability of coalescence of microvoids formed as a result of a debonding phenomenon, into a major crack spanning the entire sample cross-section. Hence, in the strain interval from ε^* to ε_b the deficit of the specific internal energy change in filled samples as compared to the neat matrix polymer, $\delta(\Delta U/m)$, can be equated to the heat released due to the creation of a free (debonded) filler surface, i.e.,

$$\partial(\Delta U/m) \approx f\varphi\gamma_{12}S_{12}, \qquad (2)$$

where $\gamma_{12} = \gamma_{12}^0 + \gamma_{12}^{in}$, γ_{12}^0 is the "true" excess interfacial energy (heat of wetting), γ_{12}^{in} is the contribution of plastic flow preceding the debonding, S_{12} is the total polymer/filler interfacial area, and f is the fraction of a debonded interface.

The values of $\delta(\Delta U/m)$ and φ are known from the experiment $S_{12} \approx 3 \times 10^5$ cm^2/g is the tabulated value of the specific surface area of Kaolin particles [20]. Hence, there are only two unknowns in the r.h.s. of Equation 2, namely, f and γ_{12}. As a crude approximation, $\gamma_{12}^0 \approx 100 \times 10^{-7}$ J/cm^2 can be assumed as a representative value for the heat of wetting of clays by paraffins (this latter value corresponds to about 20% of the heat of wetting of clays by water [20]. The contribution of γ_{12}^{in} can be estimated as $\gamma_{12}^{in} \approx \Delta H^{in} L$, where $\Delta H^{in} = 3.8$ J/g $= 3.5$ J/cm^3 is the latent heat of HDPE plastic flow [17], $L = 2r[(\varphi^*/\varphi)^{1/3} - 1]$ is the mean surface-to-surface interparticle distance [19] (i.e. the matrix ligament thickness [21], and $\varphi^* = 0.60$ (see above).

In spite of rather drastic assumptions referred to above, the absolute values of f at a fixed strain $\varepsilon = 0.07 > \varepsilon^*$ calculated in this fashion (Table I) seem quite reasonable. Therefore, the increasing difference between $\Delta U/m$ curves for filled and unfilled samples of both series at still higher strains can be explained by further progress of the debonding process (i.e., by the increase of parameter f in Equation 2).

4. Conclusions

1. The crystallinity of the HDPE matrix in the filled samples remains essentially the same as that in the neat polymer regardless of the filler content.

2. The thermoelastic behaviour of all samples in the strain interval below the apparent yield point ε^* can be quantitatively described by means of classical equations for elastic solids.

3. Thermoelastic parameters of the boundary interphase (BI) offering the best fit to predictions of the step-by-step averaging approach imply an unusually stiff, highly oriented structure of the matrix polymer within BI.

4. The difference between experimental values of the internal energy increment in the inelastic strain interval above ε^*, for the unfilled and filled samples, respectively, can be explained by the onset and further progress of the filler debonding process.

Acknowledgements

This work was supported by the BMBF through the project UKR-031-96 and by the DGICYT, Spain (Grant

PB94-0049). Thanks are due to the Ministerio de Educacion y Cultura, Spain, for a sabbatical grant to V.P.P. Technical assistance of Drs. V. I. Shtompel and V. V. Korskanov in the X-ray experiments and in the elaboration of the computer program for treatment of thermoelastic data by the SSA approach, respectively, is gratefully acknowledged.

References

1. R. WALTER, K. FRIEDRICH, V. PRIVALKO and A. SAVADORI, *J. Adhesion* **64** (1997) 87.
2. E. G. PRIVALKO, A. V. PEDOSENKO, V. P. PRIVALKO, R. WALTER and K. FRIEDRICH, *J. Appl. Polym. Sci.*
3. A. SAVADORI, M. SCAPIN and R. WALTER, *Eurofillers '95*, France, Macromolecular Symposia, Vol. 108 (1996) 183.
4. YU. S. LIPATOV, V. V. SHILOV, YU. P. GOMZA and N. E. KRUGLYAK, "X-Ray Methods of Characterization of Polymer Systems" (Naukova Dumka, Kyiv, 1982) (in Russian).
5. E. I. ORANSKAYA, X-ray studies of the structure of segmented polyurethanes, PhD thesis, Institute of Macromolecular Chemistry, National Academy of Sciences of Ukraine, 1991 (in Russian).
6. F. J. BALTA CALLEJA, *Adv. Polymer Sci*. **66** (1985) 117.
7. C. SANTA CRUZ, F. J. BALTA CALLEJA, H. G. ZACHMANN, N. STRIBECK and T. ASANO, *J. Polym. Sci. Phys.* **29** (1991) 819.
8. L. I. MIRONTSOV, Thermodynamics of deformation of segmented polyurethanes, PhD thesis, Institute of Macromolecular Chemistry, National Academy of Sciences of Ukraine, Kyiv, 1987.
9. A. I. TREGUB, Thermodynamics of deformation of polymer composites in the simple shear regime, PhD thesis, Institute of Macromolecular Chemistry, National Academy of Sciences of Ukraine, Kyiv, 1990.
10. A. I. TREGUB, V. P. PRIVALKO, H.-G. KILIAN and G. MAROM, *Appl. Compos. Mater*. **1** (1994) 167.
11. A. TREGUB, H.-G. KILIAN and J. KARGER-KOCSIS, *Compos. Interfaces* **3** (1996) 333.
12. B. WUNDERLICH, "Macromolecular Physics," Vol. 1 (Academic Press, New York, 1973).
13. F. J. BALTA CALLEJA and C. G. VONK, "X-Ray Scattering of Synthetic Polymers" (Elsevier, Amsterdam, 1989).
14. F. J. BALTA CALLEJA and H.-G. KILIAN, *Colloid & Polym. Sci*. **263** (1985) 697.
15. Physical and Optical Properties of Minerals, in "CRC Handbook of Chemistry and Physics," edited by D. R. Lide (CRC Press, Boca Raton, 1996).
16. D. TABOR, "The Hardness of Metals" (Oxford C. Press, 1951).
17. YU. K. GODOVSKY, "Thermophysical Properties of Polymers" (Springer Verlag, Berlin, 1992).
18. H. S. KATZ and J. V. MILEWSKI, "Handbook of Fillers for Plastics" (Van Nostrand Reinhold, New York, 1987).
19. V. P. PRIVALKO and V. V. NOVIKOV, "The Science of Heterogeneous Polymers" (Wiley, Chichester, 1995).
20. H. VAN OLPHEN, in "Surface Area Determination," edited by D. H. Everett and R. H. Ottewill (Butterworths, London, 1970).
21. S. WU, *J. Appl. Polym. Sci*. **35** (1988) 549.

Received 28 July
and accepted 28 September 1998